Pędziwiatr-Werbicka, E. et al. (2021) 'Evaluation of dendronized gold nanoparticles as siRNAs carriers into cancer cells', Journal of molecular liquids, 324, p. 114726.

Available at https://doi.org/10.1016/j.molliq.2020.114726

(Article begins on next page)

Evaluation of dendronized gold nanoparticles as siRNAs carriers into cancer cells

Elżbieta Pędziwiatr-Werbicka a,∗, Michał Gorzkiewicz a,∗, Sylwia Michlewska b, MaksimIonova, Dzmitry Shcharbin c, Barbara Klajnert-Maculewicz a,d, Cornelia E. Peña-Gonzáleze,f,g, Javier Sánchez-Nieves e,f,g, Rafael Gómez e,f,g, F. Javier de la Mata e,f,g, Maria Bryszewska,a

a University of Lodz, Faculty of Biology and Environmental Protection, Department of General Biophysics, 141/143 Pomorska St., 90-236 Lodz, Poland

b University of Lodz, Faculty of Biology and Environmental Protection, Laboratory of Microscopic Imaging and Specialized Biological Techniques, 12/16 Banacha St., 90-237 Lodz, Poland

c Institute of Biophysics and Cell Engineering of NASB, 27 Akademicheskaya St., 220072 Minsk, Belarus

d Leibniz Institute of Polymer Research Dresden, 6 Hohe St., 01069 Dresden, Germany

e Department of Organic and Inorganic Chemistry and Research Chemistry Institute "Andrés M. del Río" (IQAR), University of Alcalá, 28871 Alcalá de Henares, Spain

f Networking Research Center for Bioengineering, Biomaterials and Nanomedicine (CIBER-BBN), 28029 Madrid, Spain

g Institute "Ramón y Cajal" for Health Research (IRYCIS), 28034 Madrid, Spain

ABSTRACT

Gene therapy is one of the most promising approaches for potential application in the treatment of diseases, ranging from cancer and heritable disorders to infectious diseases. Before nucleic acid molecules can reach their site of action inside target cells, theymust overcome several obstacles. Thus, to fully exploit the therapeutic potential of nucleic acids, efficient delivery systems are required. We herein evaluated gold nanoparticles (AuNPs) covered with cationic carbosilane dendrons as siRNA delivery systems. Detailed analysis of formation of AuNP:siRNA complexes using circular dichroism, zeta-potential, zeta-size, electronmicroscopy and gel electrophoresiswas performed. The stability of complexes in presence of heparin and RNasewas evaluated. Internalization of AuNPs and their complexes with siRNAs into cancer cells was estimated by ultrastructure analysis and confocal microscopy. The cytotoxicity of dendrons, AuNPs and their complexes with siRNAs on 4 cancer cell lines (Caco-2, HeLa, U937 and THP-1)was estimated.We concluded that dendronization of AuNPs is a promising way to develop siRNA carriers for anticancer gene therapy.

Keywords: Dendron; Gold nanoparticle; siRNA; Anticancer gene therapy

1. Introduction

The use of nucleic acids as therapeutic agents to modulate gene and protein expression may give rise to powerful tools, with important benefits in biology and medicine [1–3]. However, one of the main limitations in the development of efficient treatment method in the field of gene therapy concerns delivery. Before nucleic acid molecules can reach their site of action inside target cells, they must overcome several obstacles, mainly due to their negative Surface charge and structural properties, low stability, and susceptibility to enzymatic degradation; these factors affect the time of systemic circulation, impede the overcoming of tissue barriers, and hamper efficient intracellular delivery and accumulation [4,5]. Thus, in order to fully exploit the therapeutic potential of nucleic acids, efficient delivery systems are required. In general, the delivery devices used to introduce nucleic acids into the cells can be divided into viral and non-viral carriers [6]. Viruses functioning as natural gene delivery vehicles due to their innate mechanisms of introduction of DNA and RNA into the cells were initially the most legitimate choice for achieving efficient transfection. However, high costs of production, low cargo capacity and the adverse side effects associated with induction of immune responses or undesired insertional mutagenesis may hamper the positive outcome of the therapy, significantly limiting the use of this type of carrier [7,8]. Thus, much effort has been paid to the elaboration of synthetic, non-toxic and nonimmunogenic carriers of appropriate size and surface charge, along with the capacity to protect nucleic acids from degradation (which

is usually due to complexation or encapsulation in the structure of the vehicle), prolonged circulation time, efficient cellular uptake and endosomal escape, as well as the ability to release the cargo intracellularly in order to enable the interactions with its targets [9–11]. Compounds, such as cationic lipids, cyclodextrins or dendritic polymers proved to be effective in overcoming the limitations of viral vectors [1,9,12], although their application, despite high transfection efficacy and facile production, remains limited due to their low storage stability, weak targeting potential and difficult in vivo tracking.

Thus, in order to improve efficient delivery system for nucleic acids, the attention has been focused on gold nanoparticles (AuNPs) [13]. Current studies confirm several advantages of nanogold over different nanomaterials, primarily due to highly optimized methods of synthesis of AuNPs of numerous sizes and shapes, featuring unique physicochemical properties [13,14].

The transport of nucleic acids is possible through the application of non-covalent complexes with surface-modified gold nanoparticles; these formulations provide increased activity of therapeutic nucleic acids due to their protection against nuclease degradation, improved cellular uptake and enhanced endosomal escape via the “proton sponge” effect [10–12]. The strength of these effects is dependent on the AuNP:nucleic acid ratio, surface charge coverage and hydrophobicity of the nanosystems [10–12]. The strong negative charge of nucleic acids makes cationic AuNPs the most efficient in forming stable complexes with siRNA or double-stranded DNA plasmids [14]. For the purpose of generating positive surface charge, AuNPs were previously modified with quaternary ammonium, poly(ethylenimine) (PEI) or amino acids [13]. Peña-González et al. [15,16] synthesized watersoluble dendronized cationic AuNPs and characterized their physicochemical (using 1H NMR, TEM, DLS, TGA and UV), biological (hemolysis, platelets aggregation and lymphocyte proliferation), antibacterial and antifungal

properties. The role of cationic carbosilane dendrons andmetallic core of functionalized gold nanoparticles in their interaction with human serum albumin [17] and alpha-1-microglobulin [18] was studied.

Here, we have focused on the impact of dendronization of AuNPs on their interactionswith small interfering RNAs (siRNAs) directed against anti-apoptotic proteins of BCL family, commonly overexpressed in various tumors.We characterized the biophysical and biological properties of non-covalent AuNP:siRNA complexes,which allowed us to perform a preliminary evaluation of the applicability of AuNPs capped with cationic carbosilane dendrons in anticancer therapy.

2. Materials and methods

2.1. Dendrons and gold nanoparticles

The synthesis and characteristics of dendrons (named 7, 8, 9) and dendronized gold nanoparticles (named 13, 14, 15 respectively) (Fig. 1) are presented in paper [15] and its supplementary materials. To study the effect of AuNP dendronization, the molar concentration of AuNPs herein is that of the corresponding dendron attached to the core.

2.2. siRNAs

The following non-fluorescent and FITC-labeled siRNAs (Dharmacon Inc., USA) directed against anti-apoptotic proteins of BCL family were used: siBcl-xl (Sense: 5'C.A.G.G.G.A.C.A.G.C.A.U.A.U.C.A.G.A.G.dT.dT3' Antisense: 5'C.U.C.U.G.A.U.A.U.G.C.U.G.U.C.C.C.U.G.dT.dT3'), siMcl-1 (Sense: 5'G.G.A.C.U.U.U.U.A.U.A.C.C.U.G.U.U.A.U.dT.dG3' Antisense: 5' A.U.A.A.C.A.G.G.U.A.U.A.A.A.A.G.U.C.C.dT.dG3')

2.3. Cell culture

HeLa (cervix adenocarcinoma), CaCo-2 (colorectal adenocarcinoma), THP-1 (acute monocytic leukemia) and U937 (histiocytic Fig. 1. Structure of AuNPs and corresponding dendrons. lymphoma) human cell lines were purchased from ATCC (Manassas, USA) and maintained under standard conditions in DMEM (HeLa, CaCo-2) or RPMI-1640 (THP-1, U937) Medium (Thermo Fisher Scientific, USA) supplemented with 10% fetal bovine serum, penicillin (100 U/ml) and streptomycin (100 μg/ml) (Sigma-Aldrich, USA) at 37 °C in an atmosphere of 5% CO2. Cells were sub-cultured 2–3 times per week.

2.4. Reagents

Buffer solution containing 10 mmol/l Na-phosphate buffer and 140 mmol/l of NaCl, pH 7.4 (PBS) and other reagents were purchased from Sigma Aldrich (USA). The buffer was passed through a 0.22 μm filter to remove trace particles.

2.5. Gel electrophoresis

Agarose gel electrophoresis was used to analyze the formation of complexes between nanoparticles and siRNAs, since positively charged nanoparticles prevent negatively charged

siRNA from migration in an electric field. Gel electrophoresis was also used to check whether AuNPs protect siRNA from ribonucleolytic degradation. Nanoparticles were complexed with siBcl-xl (1.5 μM) in different molar ratios. Complexes were incubated for 20 min at room temperature (RT) in 10mmol/l PBS. Complex formation was assessed by the retardation of migration of the siRNAs during electrophoresis for 35 min at 60 mA in a 3% agarose gel containing GelRed stain. After electrophoresis, the gel was visualized using UV light and a digital photograph of the stained gel was taken.

To check the protective effect of AuNPs against siRNA degradation, AuNP:siRNA complexes in molar ratio 300 for dendron 7; 20 for dendron 8; 10 for dendron 9 and 40 for AuNP13; 15 for AuNP14; 8 for AuNP15, and siRNA alone were treated with RNase A (1.25 μg/ml) for 45 min at 37 °C. Heparin (0.082 mg/ml) was added to the samples and incubated on ice for 5 min to check whether siRNA was protected from digestion by RNase A.

2.6. Zeta potential and particle size

The zeta potential of nanoparticles (dendrons and dendronized gold nanoparticles) and nanoparticle:siRNA complexes was determined by their electrophoretic mobility using the Smoluchowski approximation on Zetasizer Nano S90 (Malvern Instruments). Complexes were prepared in PBS by mixing 0.25 μmol/l siRNA (siBcl-xl/siMcl-1) with Fig. 2. Analysis of the formation of AuNP:siRNA complexes between siBcl-xl and dendrons or dendronized AuNPs. AuNPswere complexedwith siRNA in 10mmol/l PBS, pH 7.4. Complexes were analyzed by electrophoresis in 3% agarose gels, with siRNA migration identified by siRNA staining. The complexes were formed in different AuNP:siRNA molar ratios. AuNP molar concentration is the concentration of the corresponding dendron attached to the core. The first lane shows the migration of non-complexed siRNA. Increasing concentrations of nanoparticles (differentmolar ratios of NP:siRNA). The zeta potential of a sample was determined at 37 °C from 3 independent repetitions (8 measurements for each one). The hydrodynamic diameters of particles (dendrons and dendronized gold nanoparticles) and AuNP:siRNA complexes were measured by dynamic light scattering (DLS) using a Zetasizer Nano S90 (Malvern Instruments Ltd., UK) at 37 °C. Light scattered at 90° from the incident light was fitted to an autocorrelation function using the method of cumulants (Malvern Instruments Ltd., UK). Complexes were prepared bymixing 0.25 μmol/l siRNA with nanoparticle for 20 min in various molar ratios of nanoparticle: siRNA. The particle size was determined from3 independent repetitions- the average of 8 cycles in Malvern disposable plastic cuvettes. The particle size distribution was determined using multimodal peak analysis by intensity. When polydispersity index PDI was <0.5, the Z-average was taken into account; when the PDI was >0.5, peaks were analyzed.

2.7. Circular dichroism

CD spectra of nanoparticle:siRNA complexes were measured with a Jasco J-815 CD spectrometer (JASCO International Co., Ltd., Tokyo, Japan). Concentrations of nanoparticles increased over the experimentand concentration-dependent measurements were made in a 10 mmol/l Na-phosphate buffer (pH 7.4). Samples in the final nanoparticle:siRNA molar ratio were also treated with 0.164 mg/ml heparin. CD spectra were obtained between 320 and 200 nm in a 0.5 cm pathlength Helma quartz cell. The recording parameters were as follows: scan speed - 50 nm/min, step resolution - 0.5 nm, response time - 4 s, bandwidth - 1.0 nm, and slit -

auto. Spectra are given as the average of at least 3 independent scans. CD spectra were corrected against the baseline with the nanoparticles dissolved in buffer without siRNA. The mean residue ellipticity Θ [18,19] expressed as cm2dmol−1, was calculated using software provided by Jasco. Themaximum ellipticity values for free siRNA (Θ0) and for siRNA with nanoparticles (Θs) were calculated and plotted on the graph as a function of the nanoparticle:siRNA molar ratio [19,20].

2.8. Transmission electron microscopy

TEM was used to analyze size and morphology of siRNA, gold nanoparticles and nanoparticle:siRNA complexes. Specimens for TEM were prepared by dropping the solutions onto a 200-mesh carbon coated copper grids. After drying and staining with 2% uranyl acetate (in the case of siRNA and complexes) for 20 min, they were examined in JEOL JEM – 1010 (JEOL Ltd., Tokyo, Japan) electron microscope at 80 kV. TEM assay was also used to analyze ultrastructural changes of HeLa cells. The cells were treated with 4 µmol/l AuNP13 and its complex with siRNA for 24 h. After incubation, cells were washed twice with PBS and fixed with 2.5% glutaraldehyde for 2 h. The cells were scraped off, dispersed in 1.5% agarose and rinsed 3 times with the same buffer. The cells were post-fixed in 1% osmium tetroxide for 2 h at 4 °C, and dehydrated in ethanol and propylene oxide before being embedded in Epon-Spur's resin mixture. Samples were sectioned on an Ultra-cut E (Reihert Jung, Germany) ultramicrotome with a diamond knife. Sections (70–80 nm) were placed on formvar-coated nickel grids (300 mesh) and cell ultrastructure was examined with TEM.

2.9. Confocal microscopy

To assess the internalization of AuNP:siRNA complexes into cancer cells (HeLa) confocal microscopy was used. Sterile glass cover slips were placed in a 24-well plate. HeLa cells were seeded at 5 × 104 cells/ml by adding 400 µl per well. Cells were incubated for 24 h at 37 °C. Subsequently, the cells were treated with 100 µl solution of AuNP: siRNA complexes (prepared in molar ratios with slightly positive zeta potential, preincubated for 20 min). After incubation for 3 h under the same conditions, cells were prepared for staining. Cells were washed with 0.1% BSA solution in PBS 3 times (to avoid background signal). A 10% formalin solution was added for 5 min and the cells were rinsed with PBS before being treated for 5 min with 0.1% Triton X-100. After washing with PBS, cells were incubated with 5% BSA for 30 min. Primary antibody was added (RAB9 Monoclonal Antibody, Thermo Fisher Scientific, USA) at a ratio of 1:100 (prepared in PBS with 1% BSA). After 4 h, cells were washed with PBS before the secondary antibody CFTM633 (Biotium, USA) at a concentration of 6 µg/ml prepared in PBS with 1% BSA was added and incubated for 1 h. After washing with PBS, cells were incubated with 4 µg/ml DAPI solution for 5 min. Cells were rinsed with PBS and treated for 20 min with Phalloidin CF™ 405 (Biotium, USA) at RT. Finally, after washing with PBS, cells were mounted on coverslips with mounting solution and kept at 4 °C. Images were taken with a Leica TCS SP8 microscope (Leica Microsystems GmbH, Germany) at different wavelengths (405, 495 and 565 nm). Leica software was applied to analyze the data.

2.10. Cytotoxicity assay

The resazurin assay was used to estimate the cytotoxic activity of tested compounds. Cells were seeded into 96-well black plates at 1 × 104 cells per well and treated with increasing concentrations of AuNPs and dendrons (in a dendron concentration range 0.8–100 μM) for 3 and 24 h. Following incubation, resazurin was added to the culture medium at 10 μg/ml and the plates incubated at 37 °C in darkness to allow conversion of resazurin to resorufin. Fluorescence of metabolized resazurin in the cell suspension wasmeasured after 30 and 90 min at 530 nm excitation and 590nmemission using PowerWave HTMicroplate Spectrophotometer (BioTek, USA). Cell viability was calculated as the increase in resorufin fluorescence between 30 and 90 min. IC50 values were calculated using GraphPad Prism 8 software.

The cytotoxicity of siRNA and complexes formedwith AuNP15 were determined in an analogous manner. The complexes were prepared in PBS in 5:1 and 10:1 AuNP:siRNA molar ratios. The AuNP concentration in the complexes was constant and equal to AuNP15 IC50 for each cell line tested. The mixtures were incubated for 30 min at RT to allow the formation of complexes. The compounds were subsequently added to the cells and the resazurin assay was run after 24 h of incubation.

2.11. Statistics

Formultiple comparisons, ANOVA followed by Newman-Keuls posthoc test was applied. In all tests, p values <0.05 were considered to be statistically significant.

3. Results

3.1. Gel electrophoresis

Fig. 2 shows the gels with different patterns of migration of siBcl-xl depending on the type of nanoparticle used for complexation. Complexes were formed in different AuNP:siRNA molar ratios with siRNA being mixed with increasing concentrations of dendrons (Fig. 2 left panels, Table 1) or dendronized AuNPs (Fig. 2 right panels, Table 1).

Table 1
Molar ratios of complexes formed by nanoparticles and siRNA, estimated by gel electrophoresis.

den7: siRNA	AuNP13: siRNA	den8: siRNA	AuNP14: siRNA	den9: siRNA	AuNP15: siRNA
300:1	40:1	30:1	15:1	10:1	7.5–10:1

It is clearly seen that binding to AuNP (formation of complexes) preventsmigration of siRNAs in the gel. Comparing themolar ratios of complexes, we noticed that the increase of the dendron generation (size) led to more similarities in the effect of pure dendron and dendronized AuNP. Finally, in the case of AuNP15, the core has an insignificant impact on the stoichiometry of the complexes formed.

To test a possible protective effect of AuNPs towards siRNA against degradation by RNase, agarose gel electrophoresis was used. Naked siRNA was completely digested in the presence of

RNase A (Fig. 3, second lane). When siRNA was incubated with AuNP, treatment with RNase did not cause degradation, since addition of heparin led to the release of nucleic acid from the complex (Figs. 3 and 4).

3.2. Zeta potential and particle size

Fig. 5 demonstrates that the zeta potential of all the studied complexes changed fromnegative values (for lower nanoparticle concentration) to positive values (for higher nanoparticle concentration). In all cases the zeta potential of complexes reached a plateau at the value of the zeta potential of pure AuNP. This may indicate that siRNA can be bound between AuNP branches, leaving their ends free. The molar ratios of participants obtained from zeta potential measurements are in good agreement with those obtained from gel electrophoresis. There is a difference between complexes formed by dendrons with siBcl-xl and with siMcl-1. Despite the same number of nucleotides (number of negative ions), changes in the zeta potential of siBcl-xl and siMcl-1 as a function of concentration of dendron are not uniform. This may be due to the different sequences of nucleotides in siRNAs and hence their different structures.

The hydrodynamic diameter of complexes between siRNAs and dendrons or AuNPs in PBS ranged between 120 and 800 nm, depending on dendron generation (Fig. 6). Peña-González et al. [15] showed that the hydrodynamic diameters of dendrons/AuNP in water were smaller. In buffers, nanoparticles alone and in complexeswith nucleic acids/proteins form agglomerates and aggregates with bigger hydrodynamic diameters [17,18]. The complexes formed by AuNP14 had the smallest hydrodynamic diameter of 300–400 nm. Values of hydrodynamic diameters obtained for AuNP13 and AuNP15 complexes reached 500–800 nm. In case of all studied compounds, the hydrodynamic diameter increased when the molar ratio of the complex was similar to that estimated by electrophoresis. For lower ratios, the diameter of the complex was close to that of free nanoparticle.

3.3. Circular dichroism

Circular dichroism was used to examine the effect of the nanoparticles on the secondary structure of siRNA (siBcl-xl). CD spectra were recorded over the range of 200–320 nm. The results in Figs. 7 and 8 show that the studied nanoparticles significantly changed the shape of the CD curves. Changes in the CD signal intensity of siBcl-xl depended on the increased nanoparticle concentration. This leads to the inference that dendrons (7–9) and AuNPs (13–15) gradually bind to siRNA until siRNA saturation is reached.

Heparin treatment of saturated complexes gave CD spectra similar to those of free siRNA, an effect that was considerably weaker for dendron 9 and AuNP15 (Fig. 9).

3.4. Transmission electron microscopy

TEM was used to analyze size and morphology of siRNA, gold nanoparticles alone and in nanoparticle:siRNA complexes (Fig. 10). The ultrastructure of HeLa cells after 24 h incubation with AuNP13 and its complexes with anticancer siRNA (siBcl-xl) in a molar ratio of 40:1 (positive zeta potential) was analyzed (Fig. 11). Control cells had normal ultrastructure with oval, centrally located nucleus, few mitochondria and vesicles, dense cytoplasm with endoplasmic reticulum and numerous ribosomes (Fig. 11A).

After treatment with AuNP13 the ultrastructure was slightly changed. There were more vesicles, and small granular electron dense deposits were visible in some vesicles (Fig. 11B,C). Similarly, cells treated with AuNP:siRNA complexes showed little change in ultrastructure except for large electron dense granular clusters appearing during endocytosis (Fig. 11D, E).

3.5. Confocal microscopy

To evaluate internalization of complexes formed by AuNPs and FITClabeled anticancer siRNA (siMcl-1) (in themolar ratios estimated by gel electrophoresis) to cancer cells (HeLa) after 24 h treatment, confocal microscopy was used. All the complexes (visible as green spots) were efficiently taken up by cancer cells (Fig. 12). Further, the experiments carried out using FITC-labeled siBcl-xl confirmed the results of TEManalysis - the complexeswere transported inside the cells via vesicles, most probably endosomes (Fig. 13). Due to their specific staining (red points), it was possible to depict significant role of endosomes in cellular uptake of complexes (indicated by the yellow/orange merge of green FITC-siRNA and red endosomes, Figs. 12 and 13).

3.6. Cytotoxicity

We measured the cytotoxicity of AuNPs and corresponding dendrons using 4 cell lines. The data are given in Fig. 14 (for HeLa cells) and Table 2 (all cell lines tested). It can be seen that AuNP13 and dendron7 were non-toxic for all cell lines. Increase of generation led to increased cytotoxicity, with pure dendrons being more cytotoxic than the corresponding AuNPs

Based on the data of internalization of AuNP:siRNA complexes into cells (Fig. 14 and non-presented data) and based on data from CD with heparin (Fig. 9), we chose AuNP15 to test the effect of complexes of AuNP:siRNA on cell lines (Fig. 15).

Table 2
IC50 for AuNPs and corresponding dendrons for 4 cell lines: HeLa, CaCo-2, THP-1, U937. The data given are the means ± SD (n = 3).

IC50 [μM]	HeLa		CaCo-2		THP-1		U937	
	3 h	24 h	3 h	24 h	3 h	24 h	3 h	24 h
AuNP13	–	–	–	–	–	–	–	–
AuNP14	>100	39.9 ± 2.3	>100	66.1 ± 2.8	>100	50.2 ± 5.4	>100	66.6 ± 4.8
AuNP15	29.7 ± 3.1	11.6 ± 4.6	43.9 ± 3.4	12.3 ± 1.5	9.9 ± 1.2	7.9 ± 1.6	10.9 ± 1.8	10.9 ± 0.8
Dendron7	–	–	–	–	–	–	–	–
Dendron8	36.7 ± 1.5	16.3 ± 2.1	65.5 ± 6.1	24.9 ± 1.3	35.6 ± 4.4	18.7 ± 3.8	58.1 ± 2.6	26.5 ± 3.2
Dendron9	6.9 ± 0.3	5.9 ± 0.2	35.2 ± 5.5	12.1 ± 1.2	9.8 ± 1.1	5.4 ± 0.5	9.7 ± 1.2	5.4 ± 0.4

4. Discussion

Several polymers, including heparin, hyaluronic acid, chitosan, dextran, cellulose derivatives and maltose, have been proposed as surface coats for AuNPs [21]. These polymers can improve the characteristics of AuNP, including their long-term stability and solubility, thereby enhancing the hydrophilicity of the outer surface, adjusting the surface density of the shell, imparting non-immunogenicity and improving their biocompatibility [22,23]. Polymeric modification of AuNPs is important for conjugating therapeutic agents for drug delivery applications [15,24,25]. Our carbosilane dendrons have been used in anti-HIV and cancer studies to transport siRNA [26,27].

The detailed analysis of complexation between dendronized carbosilane AuNPs and siRNA showed that AuNPs formed stable complexeswithsiRNAinmolar

ratiosdependingonthegenerationof the dendrons.Heparin released siRNA fromdendrons and AuNPs. However, the most important finding is that the release was only partial for AuNP15 (Fig. 9). Even in the presence of heparin,AuNP15 could still partially interactwith siRNA. Since heparin has the highest negative charge density of the glucosaminoglycans [28] and, onthe otherhand, dendrons and dendronized AuNPs have the significant number of terminal amino groups (positive charge density), one might expect a relatively strong electrostatic interaction between dendrons, corresponding AuNPs and heparin, which could destabilize the complexes with siRNA and cause the release of the siRNAs even at low heparin concentrations.

However, AuNP15 was the most promising nanoparticle that complexed siRNA; their complex was not fully destroyed by heparin. Further, complexation of siRNA with all the dendrons and AuNPs led to protection of siRNA against RNase. Similar results were obtained for the interactions between carbosilane or PPI dendrimers and siRNAs [27,29,30].

The size of complexes depended on the method of analysis. Based on zeta-size and TEM, the size of complexes covered a wide range of 300–800 nm. Interestingly, the complexes formed by AuNP13 and 15 were larger compared to those formed by AuNP14, which may be associated with differences in size of the core and coating of nanoparticles – AuNP14 has the biggest core among studies AuNPs, with medium-sized dendrons.

Ultrastructure analysis and confocal microscopy showed the presence of AuNPs and their complexes with siRNAs inside the cells. Both methods also allowed to indicate endocytosis as the main pathway of cellular uptake of complexes, in line with previous reports [31–33].

Important data emerged from analysis of the cytotoxicity of AuNPs and their corresponding dendrons on 4 cell lines. Cytoxicity depended on the generation of dendrons, but not on the metallic core. Dendrons and dendronized AuNPs of the first generation were non-toxic for cells. Increase in the generation of dendrons led to enhanced cytotoxicity, with pure dendrons being more cytotoxic than dendronized AuNPs. This increase in the generation also enhanced the effect of dendrons and corresponding AuNPs on serum albumin and alfa-1-microglobulin [17,18]. One possible explanation involves the surface redistribution of cationic charges of dendrons at their binding to AuNPs. Such spatial distribution leads to decreased charge density of dendrons at the surface of AuNPs, a similar effect occurring with partially degraded poly(amidoamine) dendrimers [34].

The effect of complexes of AuNP:siRNA on cell lines was studied using AuNP15, chosen based on CD data with heparin and confocal microscopy. We used 2 different siRNAs: siBcl-xl against anti-apoptotic protein Bcl-xl and siMcl-1 against anti-apoptotic proteinMcl-1, belonging to the Bcl-2 family [35,36]. In complex with AuNP, siMcl-1 could efficiently affect 3 cancer cells, except for Caco-2. In contrast, siBcl-xl had little effect only on U937. The differences in the effect of siBcl-xl and siMcl-1 can be explained by the differences in their overexpression and activity in cancer cell lines [37]. In contrast to Bcl-xl, Mcl-1 protein plays a pivotal role in protecting cells from apoptosis and is overexpressed in a variety of human cancers [37–39]. Among the antiapoptotic Bcl-2 family members, only Mcl-1 is uniquely regulated by numerous oncogenic signaling pathways [40]. Bcl-xl is overexpressed in U937 cells [41], and thus the effect of siBcl-xl seen in our results.

Based on our studies, we conclude that AuNPs can efficiently form complexes with siRNAs. The stability of the complex depends on the generation of dendron, i.e. complexes with higher generations are more stable in the presence of heparin. Complexes have a hydrodynamic size of 250–700 nm and show the ability to transfect cancer cells. The effect of siRNA co-delivered with AuNP15 inside the cancer cells depended on the type of nucleic acid used: in contrast to siBcl-xl, siMcl-1 was efficient in 3 of the tested cancer cell lines. Thus, the complexes of dendronized AuNPs with anticancer siRNA may prove useful especially in case of the therapy of tumors overexpressing Mcl-1.

However, based on the analyzes performed, at this stage of research it is impossible to draw definite conclusions indicating the most promising siRNA carrier. Moreover, given the significant cytotoxicity of studied AuNPs, additional modifications may be necessary to reduce the inherent toxic activity of dendronized gold nanoparticles or to ensure targeted transport. Our research is ongoing and the panel of test compounds will be expanded to include PEGylated dendronized AuNPs to enhance the biocompatibility of the potential delivery system for nucleic acids.

CRediT authorship statement

Elżbieta Pędziwiatr-Werbicka: Conceptualization, Methodology, Investigation, Formal analysis, Data curation, Writing-original draft preparation, Writing-review and editing, Supervision, Project administration. Michał Gorzkiewicz: Formal analysis, Investigation, Writing original draft preparation, Writing-review and editing. Sylwia Michlewska: Investigation. Maksim Ionov: Investigation. Dzmitry Shcharbin: Writing-original draft preparation. Barbara Klajnert-Maculewicz: Writing-review and editing. Cornelia E. Peña-González: Synthesis of nanoparticles. Javier Sánchez-Nieves: Synthesis of nanoparticles. Rafael Gómez: Synthesis of nanoparticles. F. Javier de la Mata: Synthesis of nanoparticles. Maria Bryszewska: Writing-review and editing, Funding acquisition.

Declaration of Competing Interest

The authors declare that they have no known competing financial interests or personal relationships that could have appeared to influence the work reported in this paper.

Acknowledgements

This work was supported by the Polish National Agency for Academic Exchange, grant EUROPARTNER, No. PPI/APM/2018/1/00007/U/001; supported by grants fromCTQ2017-86224-P (MINECO), SBPLY/17/180501/000358 (JCCM), consortiums NANODENDMED II-CM ref

B2017/BMD-3703 and IMMUNOTHERCANCM B2017/BMD-3733 (CAM) to UAH CIBER-BBN as an initiative funded by VI National R-D-I Plan 2008-2011, Iniciativa Ingenio 2010, Consolider Program, CIBER Actions and financed by the Instituto de Salud Carlos III with assistance from the European Regional Development Fund; partially supported by the Belarusian Republican Foundation for Fundamental Research and State Committee of Science and Technology of Belarus, grants B19ARMG-002 and B20SLKG-002; based upon work from COST Action “Nano2Clinic. Cancer Nanomedicine - from the bench to the bedside” CA17140 supported by COST (European Cooperation in Science and Technology).

References

[1] M. Cavazzana-Calvo, A. Thrasher, F. Mavilio, The future of gene therapy, Nature 427 (6977) (2004) 779–781.

[2] L. Naldini, Gene therapy returns to centre stage, Nature 526 (7573) (2015) 351–360.

[3] C.E. Dunbar, K.A. High, J.K. Joung, D.B. Kohn, K. Ozawa, M. Sadelain, Gene therapy comes of age, Science 359 (6372) (2018) eaan4672.

[4] K.A. Whitehead, R. Langer, D.G. Anderson, Knocking down barriers: advances in siRNA delivery, Nat. Rev. Drug Discov. 8 (2) (2009) 129–138.

[5] K. Sridharan, N.J. Gogtay, Therapeutic nucleic acids: current clinical status, Br. J. Clin. Pharmacol. 82 (3) (2016) 659–672.

[6] N. Nayerossadat, T.Maedeh, P.A. Ali, Viral and nonviral delivery systems for gene delivery, Adv. Biomed. Res. 1 (2012) 27.

[7] C.E. Thomas, A. Ehrhardt, M.A. Kay, Progress and problems with the use of viral vectors for gene therapy, Nat. Rev. Genet. 4 (5) (2003) 346–358.

[8] M. Giacca, S. Zacchigna, Virus-mediated gene delivery for human gene therapy, J. Control. Release 161 (2) (2012) 377–388.

[9] T.Wang, J.R. Upponi, V.P. Torchilin, Design ofmultifunctional non-viral gene vectors to overcome physiological barriers: dilemmas and strategies, Int. J. Pharm. 427 (1) (2012) 3–20.

[10] H. Yin, R.L. Kanasty, A.A. Eltoukhy, A.J. Vegas, J.R. Dorkin, D.G. Anderson, Non-viral vectors for gene-based therapy, Nat. Rev. Genet. 15 (8) (2014) 541–555.

[11] A.B. Hill, M. Chen, C.K. Chen, B.A. Pfeifer, C.H. Jones, Overcoming gene-delivery hurdles: physiological considerations for nonviral vectors, Trends Biotechnol. 34 (2) (2016) 91–105.

[12] J. Chen, Z. Guo, H. Tian, X. Chen, Production and clinical development of nanoparticles for gene delivery, Mol. Therapy-Methods Clin. Develop. 3 (2016) 16023.

[13] E. Pedziwiatr-Werbicka, K. Horodecka, D. Shcharbin, M. Bryszewska, Nanoparticles in combating cancer: opportunities and limitations. A brief review, Curr. Med. Chem. 27 (2020) 1–13, https://doi.org/10.2174/0929867327666200130101605.

[14] K. Sztandera, M. Gorzkiewicz, B. Klajnert-Maculewicz, Gold nanoparticles in cancer treatment, Mol. Pharm. 16 (1) (2019) 1–23.

[15] C.E. Peña-González, E. Pedziwiatr-Werbicka, D. Shcharbin, C. Guerrero-Beltrán, V. Abashkin, S. Loznikova, J.L. Jiménez, M.Á. Muñoz-Fernández, M. Bryszewska, R. Gómez, J. Sánchez-Nieves, F.J. de la Mata, Gold nanoparticles stabilized by cationic carbosilane dendrons: synthesis and biological properties, Dalton Trans. 46 (27) (2017) 8736–8745.

[16] C.E. Peña-González, E. Pedziwiatr-Werbicka, T. Martín-Pérez, E.M. Szewczyk, J.L. Copa-Patiño, J. Soliveri, R. Gómez, M. Bryszewska, J. Sánchez-Nieves, F.J. de la Mata, Antibacterial

and antifungal properties of dendronized silver and gold nanoparticles with cationic carbosilane dendrons, Int. J. Pharm. 528 (1–2) (2017) 55–61.

[17] D. Shcharbin, E. Pedziwiatr-Werbicka, T. Serchenya, S. Cyboran-Mikolajczyk, L. Prakhira, V. Abashkin, V. Dzmitruk, M. Ionov, S. Loznikova, I. Shyrochyna, O. Sviridov, C.E. Peña-González, A.B. Gumiel, R. Gómez, F.J. de la Mata, M. Bryszewska, Role of cationic carbosilane dendrons and metallic core of functionalized gold nanoparticles in their interaction with human serum albumin, Int. J. Biol. Macromol. 118 (2018) 1773–1780.

[18] E. Pedziwiatr-Werbicka, T. Serchenya, D. Shcharbin, M. Terekhova, E. Prokhira, V. Dzmitruk, I. Shyrochyna, O. Sviridov, C.E. Peña-González, R. Gómez, J. Sánchez-Nieves, F.J. de la Mata, M. Bryszewska, Dendronization of gold nanoparticles decreases their effect on human alpha-1-microglobulin, Int. J. Biol. Macromol. 108 (2018) 936–941.

[19] G. Böhm, R.Muhr, R. Jaenicke, Quantitative analysis of protein far UV circular dichroism spectra by neural networks, Protein Eng. Des. Sel. 5 (3) (1992) 191–195.

[20] J.T. Yang, C.S.C. Wu, H.M. Martinez, Methods Enzymol. 130 (1986) 208–269.

[21] O.S. Muddineti, B. Ghosh, S. Biswas, Current trends in using polymer coated gold nanoparticles for cancer therapy, Int. J. Pharm. 484 (1–2) (2015) 252–267.

[22] D. Danila, E. Johnson, P. Kee, CT imaging of myocardial scars with collagen-targeting gold nanoparticles, Nanomedicine 9 (7) (2013) 1067–1076.

[23] E. Zhao, Z. Zhao, J. Wang, C. Yang, C. Chen, L. Gao, Q. Feng, W. Hou, M. Gao, Q. Zhang, Surface engineering of gold nanoparticles for in vitro siRNA delivery, Nanoscale 4 (16) (2012) 5102–5109.

[24] A. Kumar, X. Zhang, X.J. Liang, Gold nanoparticles: emerging paradigm for targeted drug delivery system, Biotechnol. Adv. 31 (5) (2013) 593–606.

[25] Y. Xiao, R. Jaskula-Sztul, A. Javadi, W. Xu, J. Eide, A. Dammalapati, M. Kunnimalaiyaan, H. Chen, S. Gong, Co-delivery of doxorubicin and siRNA using octreotide-conjugated gold nanorods for targeted neuroendocrine cancer therapy, Nanoscale 4 (22) (2012) 7185–7193.

[26] E. Pedziwiatr-Werbicka, D. Shcharbin, J. Maly, M. Maly, M. Zaborski, B. Gabara, P. Ortega, J.F. de la Mata, E. Gómez, M.A. Muñoz-Fernandez, B. Klajnert, M. Bryszewska, Carbosilane dendrimers are a non-viral delivery system for antisense oligonucleotides: characterization of dendriplexes, J. Biomed. Nanotechnol. 8 (1) (2012) 57–73.

[27] V. Dzmitruk, A. Szulc, D. Shcharbin, A. Janaszewska, N. Shcharbina, J. Lazniewska, D. Novopashina, M. Buyanova, M. Ionov, B. Klajnert-Maculewicz, R. Gómez-Ramirez, S. Mignani, J.P. Majoral, M.A. Muñoz-Fernández, M. Bryszewska, Anticancer siRNA cocktails as a novel tool to treat cancer cells. Part (B). Efficiency of pharmacological action, Int. J. Pharm. 485 (1–2) (2015) 288–294.

[28] L. Pitkänen, M. Ruponen, J. Nieminen, A. Urtti, Vitreous is a barrier in nonviral gene transfer by cationic lipids and polymers, Pharm. Res. 20 (4) (2003) 576–583.

[29] M. Ionov, J. Lazniewska, V. Dzmitruk, I. Halets, S. Loznikova, D. Novopashina, E. Apartsin, O. Krasheninina, A. Venyaminova, K. Milowska, O. Nowacka, R. Gomez-Ramirez, F.J. de la Mata, J.P. Majoral, D. Shcharbin, M. Bryszewska, Anticancer siRNA cocktails as a novel tool to treat cancer cells. Part (A). Mechanisms of interaction, Int. J. Pharm. 485 (1–2) (2015) 261–269.

[30] M. Szewczyk, J. Drzewinska, V. Dzmitruk, D. Shcharbin, B. Klajnert, D. Appelhans, M. Bryszewska, Stability of dendriplexes formed by anti-HIV genetic material and poly (propylene imine) dendrimers in the presence of glucosaminoglycans, J. Phys. Chem. B 116 (50) (2012) 14525–14532.

[31] J. Choi, Y. Rui, J. Kim, N. Gorelick, D.R. Wilson, K. Kozielski, A. Mangraviti, E. Sankey, H. Brem, B. Tyler, J.J. Green, E.M. Jackson, Nonviral polymeric nanoparticles for gene therapy in pediatric CNS malignancies, Nanomedicine 23 (2020) 102115.

[32] K.K. Hou, H. Pan, L. Ratner, P.H. Schlesinger, S.A. Wickline, Mechanisms of nanoparticle-mediated siRNA transfection by melittin-derived peptides, ACS Nano 7 (10) (2013) 8605–8615.

[33] G. Sahay, W. Querbes, C. Alabi, A. Eltoukhy, S. Sarkar, C. Zurenko, E. Karagiannis, K. Love, D. Chen, R. Zoncu, Y. Buganim, A. Schroeder, R. Langer, D.G. Anderson, Efficiency of siRNA delivery by lipid nanoparticles is limited by endocytic recycling, Nat. Biotechnol. 31 (7) (2013) 653–658.

[34] M.X. Tang, C.T. Redemann, F.C. Szoka, In vitro gene delivery by degraded polyamidoamine dendrimers, Bioconjug. Chem. 7 (6) (1996) 703–714.

[35] A. Vestin, E. Khazanov, D. Avni, V. Sergeyev, Y. Barenholz, Y. Sidi, E. Yakobson, siRNAlipoplex-mediated Bcl-2 and Bcl-xL gene silencing induces apoptosis in MCF-7 human breast carcinoma cells, Open Chem. Biomed. Methods J. 1 (1) (2008) 28–43.

[36] Q. Wang, J. Wan, W. Zhang, S. Hao, MCL-1 or BCL-xL-dependent resistance to the BCL-2 antagonist (ABT-199) can be overcome by specific inhibitor as single agents and in combination with ABT-199 in acute myeloid leukemia cells, Leuk. Lymphoma 60 (9) (2019) 2170–2180.

[37] B.A. Quinn, R. Dash, B. Azab, S. Sarkar, S.K. Das, S. Kumar, R.A. Oyesanya, S. Dasgupta, P. Dent, S. Grant, M. Rahmani, D.T. Curiel, I. Dmitriev, M. Hedvat, J. Wei, B. Wu, J.L. Stebbins, J.C. Reed, M. Pellecchia, D. Sarkar, P.B. Fisher, Targeting Mcl-1 for the therapy of cancer, Expert Opin. Investig. Drugs 20 (10) (2011) 1397–1411.

[38] H. Takahashi, M.C. Chen, H. Pham, Y. Matsuo, H. Ishiguro, H.A. Reber, H. Takeyama, O.J. Hines, G. Eibl, Simultaneous knock-down of Bcl-xL and Mcl-1 induces apoptosis through Bax activation in pancreatic cancer cells, Biochim. Biophys. Acta (BBA)-Mol. Cell Res. 1833 (12) (2013) 2980–2987.

[39] W. Xiang, C.Y. Yang, L. Bai,MCL-1 inhibition in cancer treatment, OncoTargets Therapy11 (2018) 7301–7314.

[40] M.M. Williams, R.S. Cook, Bcl-2 family proteins in breast development and cancer: could Mcl-1 targeting overcome therapeutic resistance? Oncotarget 6 (6) (2015) 3519–3530.

[41] W.L. Marshall, R. Datta, K. Hanify, E. Teng, R.W. Finberg, U937 cells overexpressing bcl-xl are resistant to human immunodeficiency virus-1-induced apoptosis and human immunodeficiency virus-1 replication, Virology 256 (1) (1999) 1–7.

FIGURES

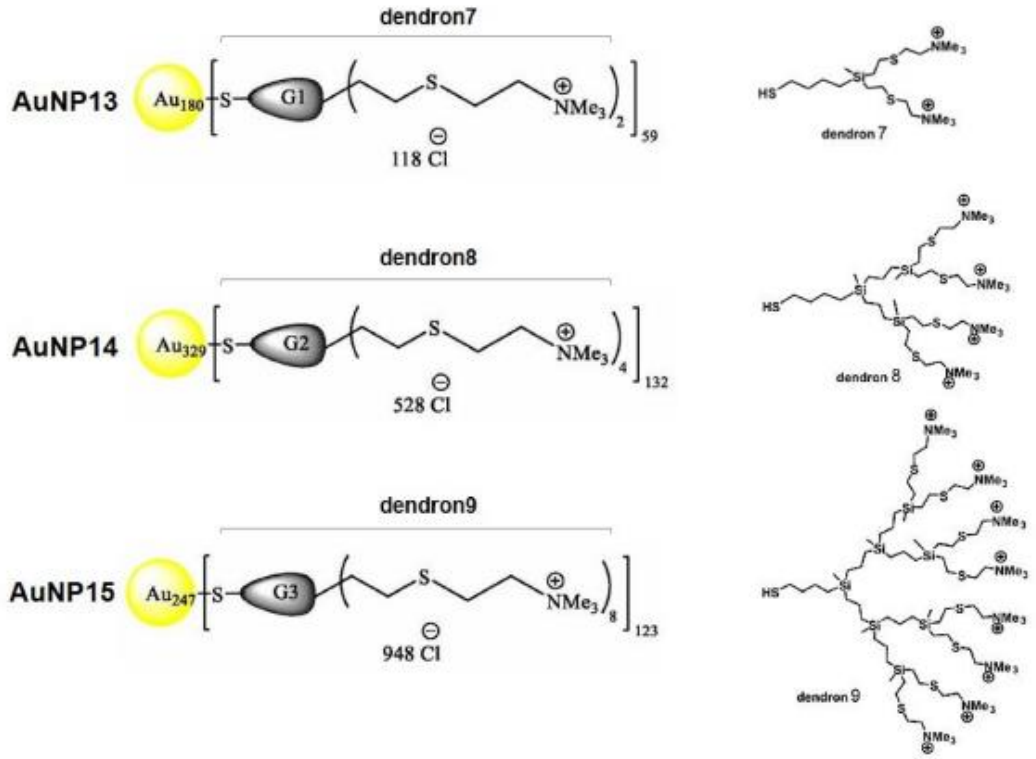

Fig. 1. Structure of AuNPs and corresponding dendrons.

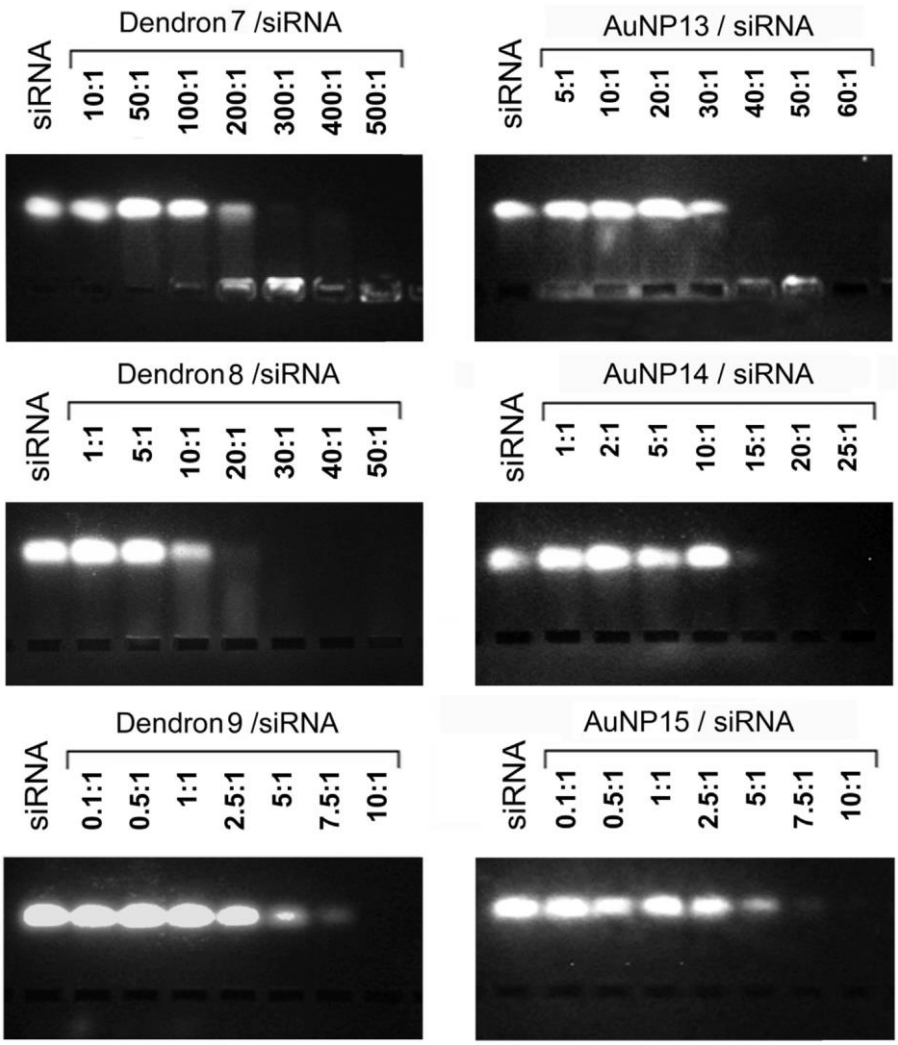

Fig. 2. Analysis of the formation of AuNP:siRNA complexes between siBcl-xl and dendrons or dendronized AuNPs. AuNPswere complexedwith siRNA in 10mmol/l PBS, pH 7.4. Complexes were analyzed by electrophoresis in 3% agarose gels, with siRNA migration identified by siRNA staining. The complexes were formed in different AuNP:siRNA molar ratios. AuNP molar concentration is the concentration of the corresponding dendron attached to the core. The first lane shows the migration of non-complexed siRNA.

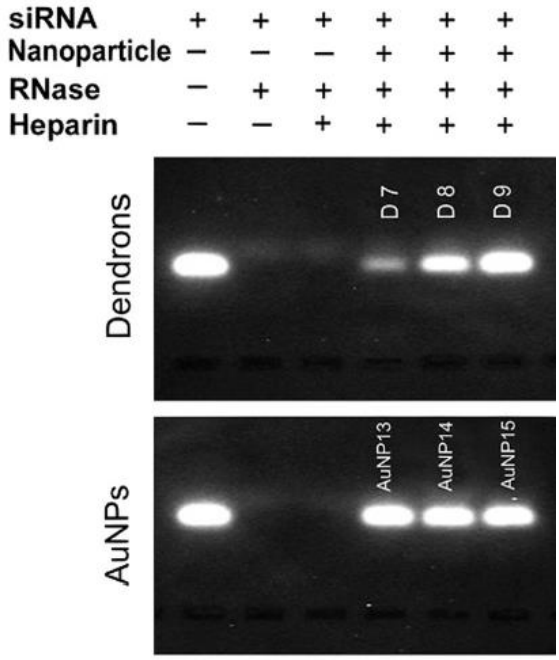

Fig. 3. Stability of complexes. Nanoparticles have a protective effect towards siRNA in the presence of RNase. Top panel: dendron 7 - (D7); dendron 8 - (D8); dendron 9 - (D9). Bottom panel: AuNP13; AuNP14; AuNP15. AuNP molar concentration is the concentration of the corresponding dendron attached to the core. The first lane shows migration of non-complexed siRNA. The second lane shows migration of siRNA previously incubated with RNase A. The third lane shows migration of siRNA previously incubated with RNase A in the presence of heparin (0.082 mg/ml). The following lanes showthemigration of siRNA due to its release fromcomplexes by heparin at 0.082mg/ml.

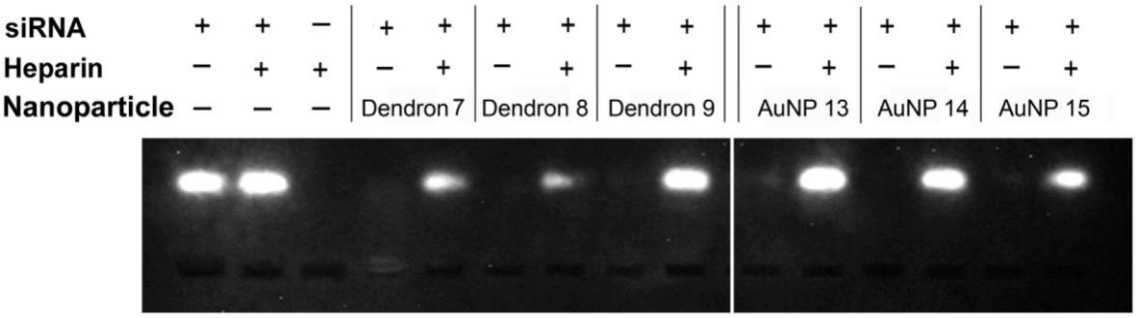

Fig. 4. Release of the siRNA fromcomplexes by addition of 0.082mg/ml heparin. The first lane showsmigration of non-complexed siRNA. The second lane showsmigration of siRNA in the presence of heparin. The third lane shows the presence of non-complexed heparin. The following lanes show the migration of siRNA due to its release from complexes after addition of heparin.

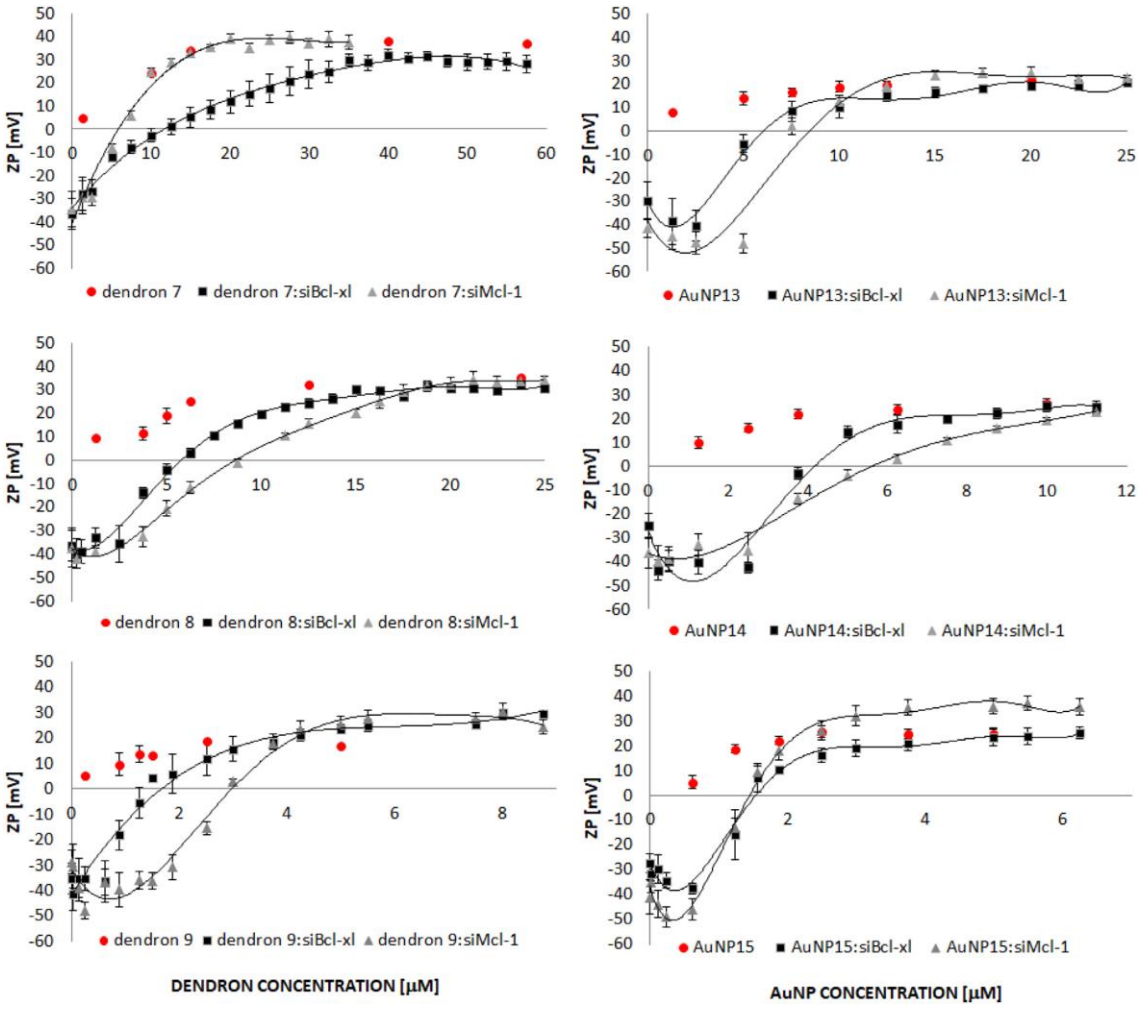

Fig. 5. Zeta potential of dendrons and dendron:siRNA complexes (left panel), AuNPs and AuNP:siRNA complexes (right panel). AuNP molar concentration is the concentration of the corresponding dendron attached to the core. [siRNA] = 0.25 µM. The data given are the means ± SD (n=3).

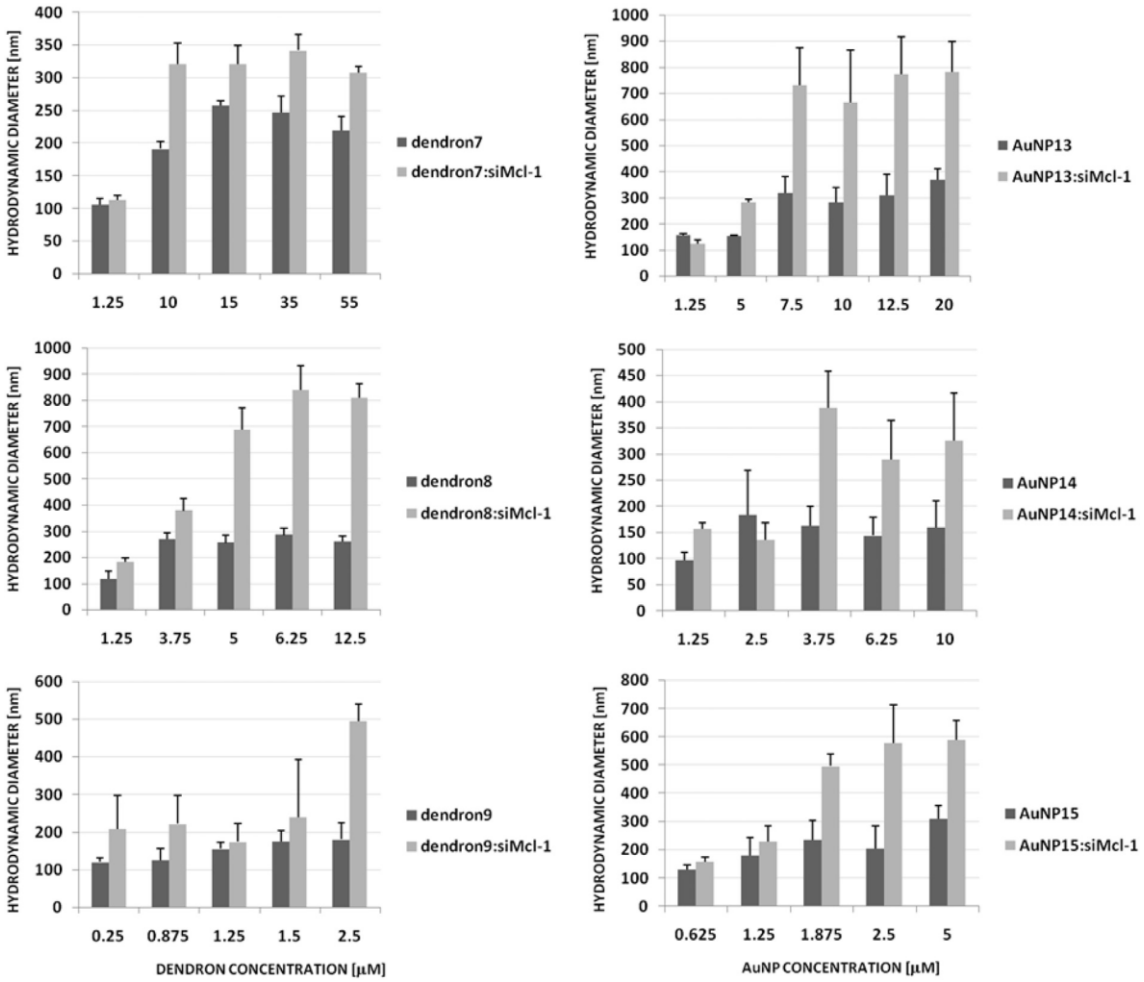

Fig. 6. Hydrodynamic diameter of dendrons and dendron:siRNA complexes (left panel), AuNPs and AuNP:siRNA complexes (right panel). AuNPmolar concentration is the concentration of the corresponding dendron attached to the core. [siRNA]= 0.25 µM. The data given are the means ± SD (n = 3).

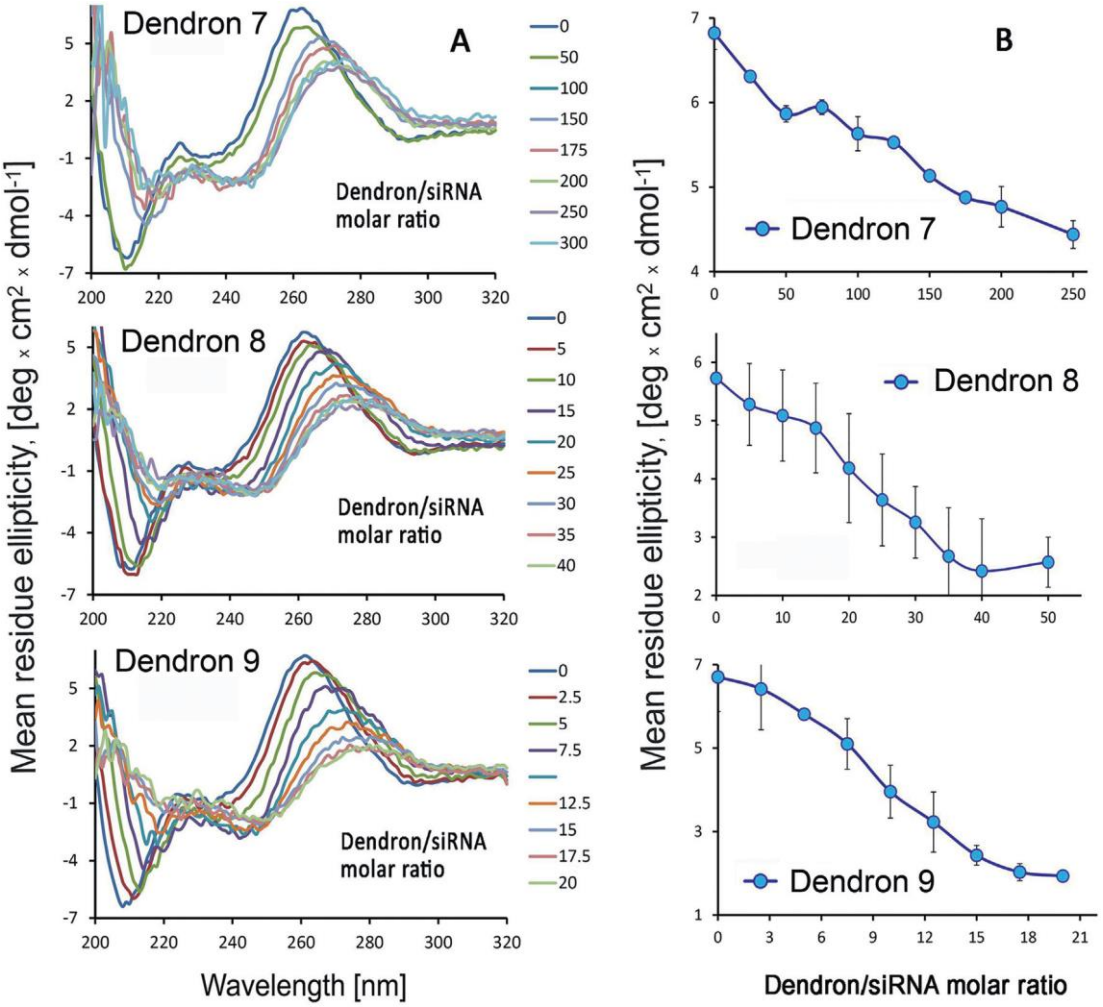

Fig. 7. (A) - CD spectra of siBcl-xl in the presence of carbosilane dendrons in increasing dendron:siRNA molar ratios. (B) - Changes in mean residue ellipticity of siBcl-xl, at λ = max 260–280 nm. The siRNA concentration was 1 μM, wavelength 200–320 nm, bandwidth 1.0 nm, response time 4 s, scan speed 50 nm/min, and step resolution 0.5 nm, using Naphosphate buffer at 10 mmol/l, pH 7.4. Results represent mean ± SD. The number of scans varied between 1 and 3 for each sample of 3 independent experiments.

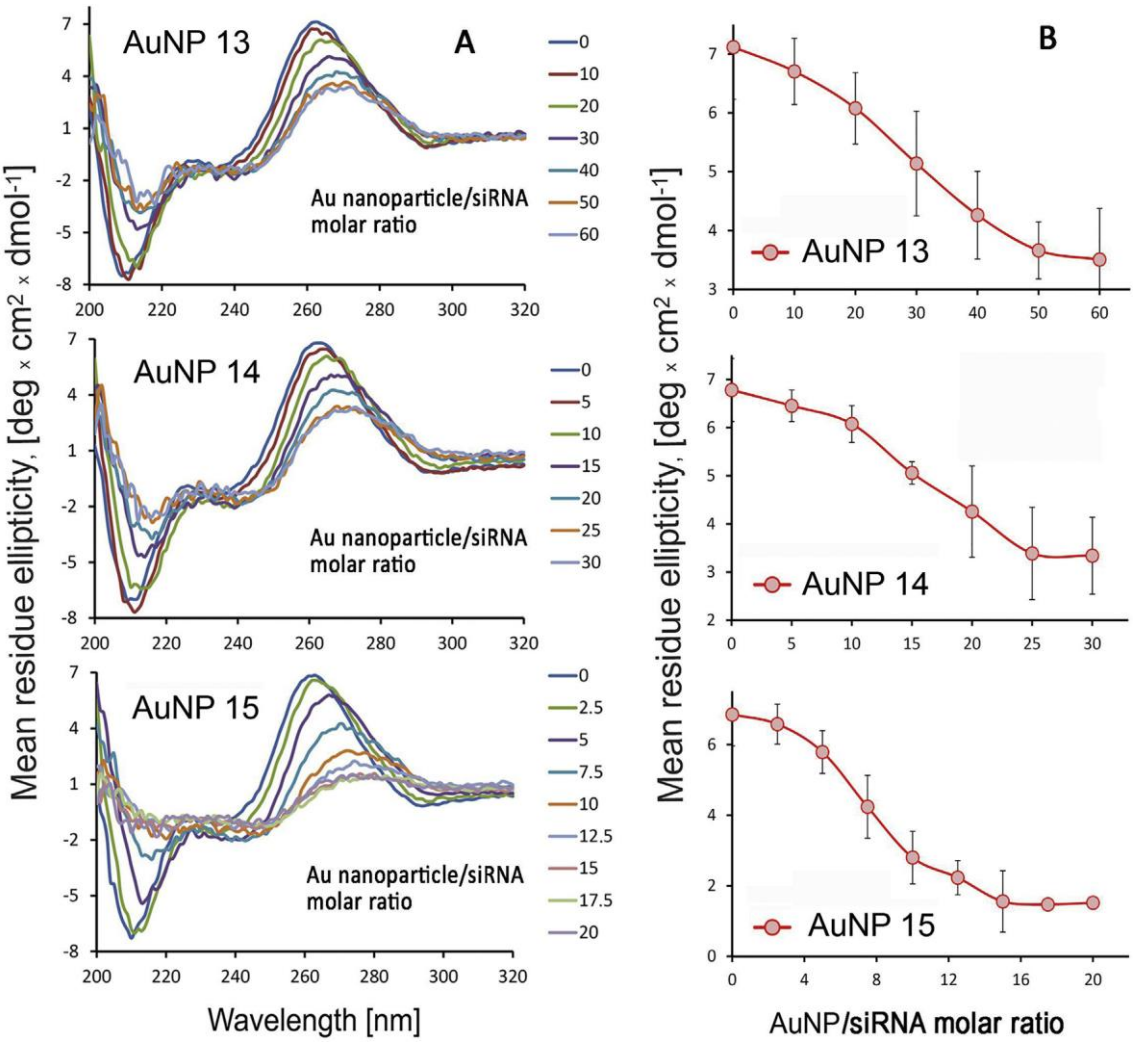

Fig. 8. (A) - CD spectra of siBcl-xl in the presence of AuNPs nanoparticles in increasing AuNP:siRNA molar ratios. AuNP molar concentration is the concentration of the corresponding dendron attached to the core. (B) - Changes in mean residue ellipticity of siBcl-xl, at λ = max 260–280 nm. siRNA concentration was 1 µM, wavelength 200–320 nm, bandwidth 1.0 nm, response time 4 s, scan speed 50 nm/min, and step resolution 0.5 nm, using Na-phosphate buffer at 10 mmol/l, pH 7.4. Results represent mean ± SD. The number of scans varied between 1 and 3 for each sample of 3 independent experiments.

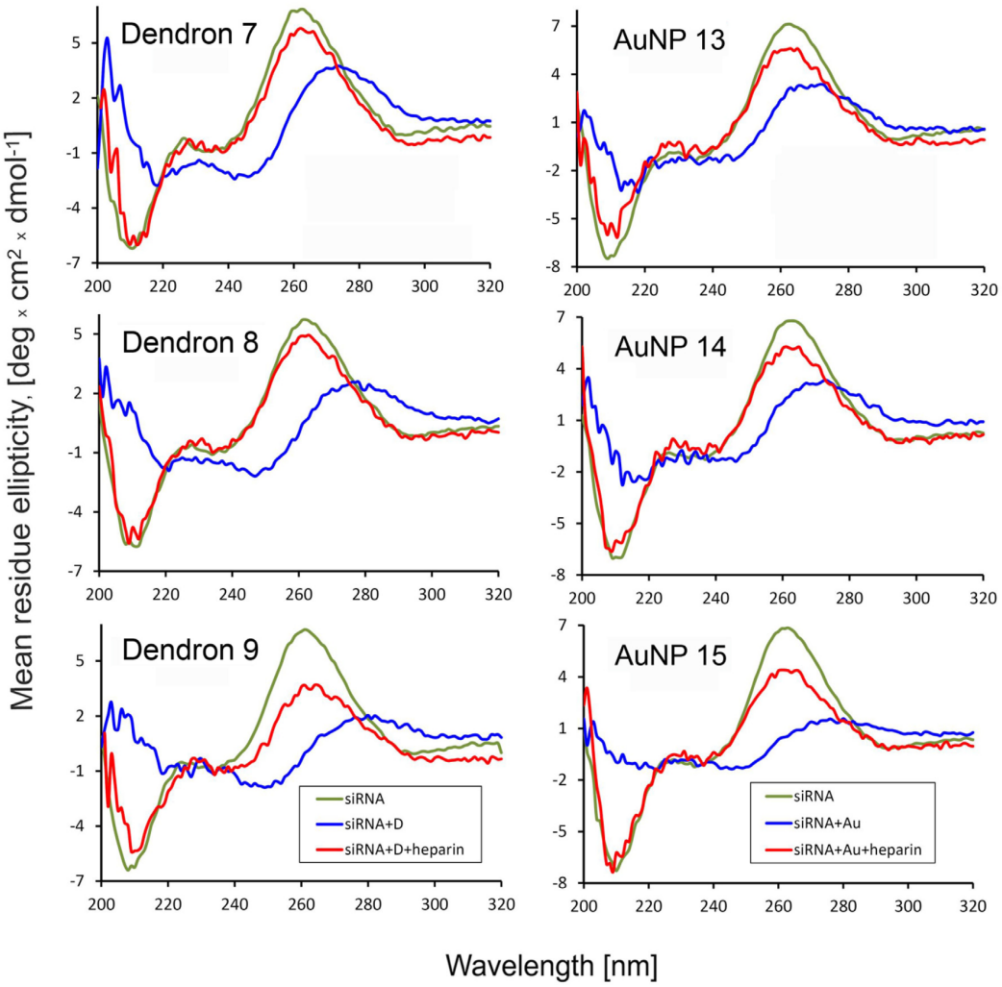

Fig. 9. CD spectra of the siBcl-xl in the presence of carbosilane dendrons (left panel) or their complexeswith AuNPs (right panel) and CD spectra of the same complexes in the presence of heparin. siRNA concentration was 1 µM,wavelength 200–320 nm, bandwidth 1.0 nm, response time 4 s, scan speed 50 nm/min, and step resolution 0.5 nm, using Na-phosphate buffer at 10 mmol/l, pH 7.4. The number of scans varied between 1 and 3 for each sample of 3 independent experiments.

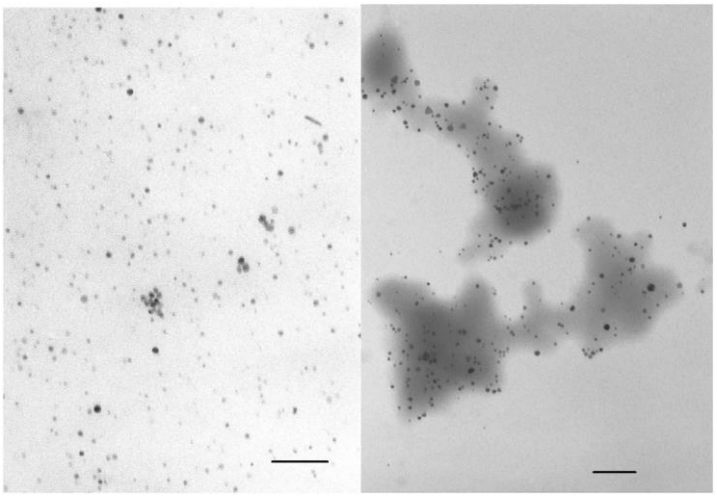

Fig. 10. TEMimages of pure AuNP13 (left) and AuNP13:siBcl-xl complex (right). Scale bar = 100 nm.

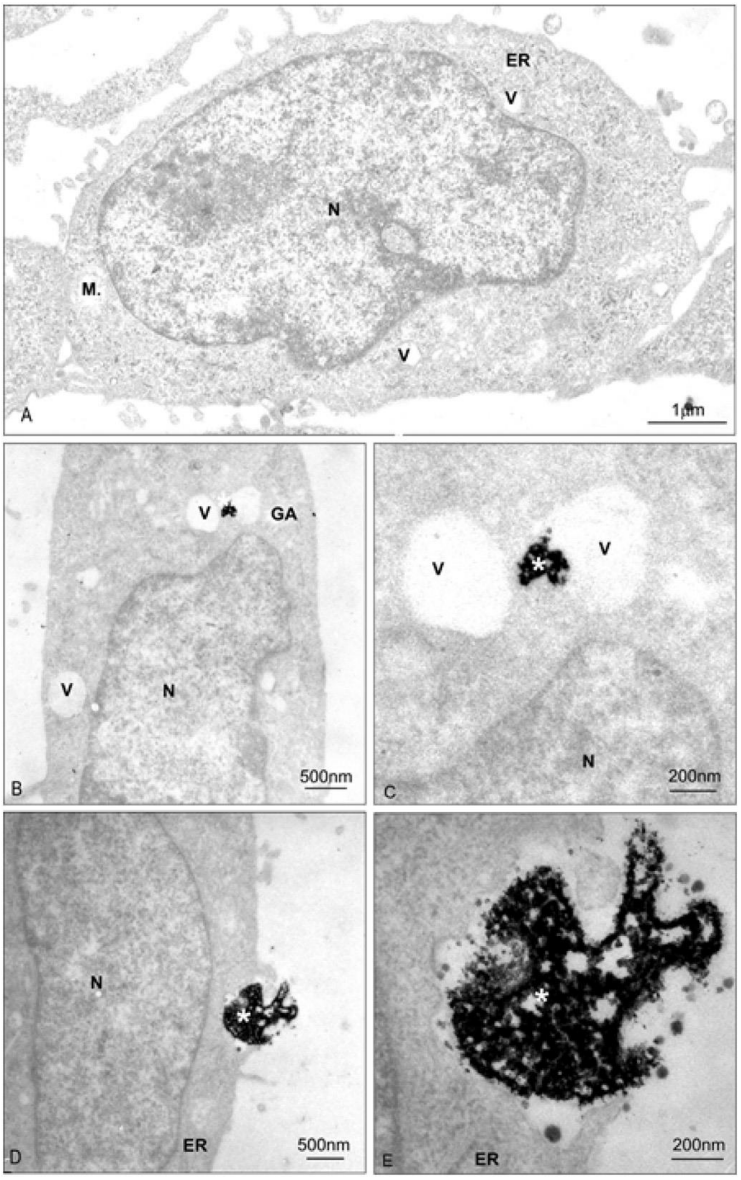

Fig. 11. Ultrastructural changes of HeLa cells (A) treated with AuNP13\\(B-C) and its complexes with siRNA (siBcl-xl) (D-E). Abbreviations: N-nucleus, M-mitochondria, GAGolgi apparatus, ER-endoplasmic reticulum, V-vesicle; * vesicle containing nanoparticles and complexes.

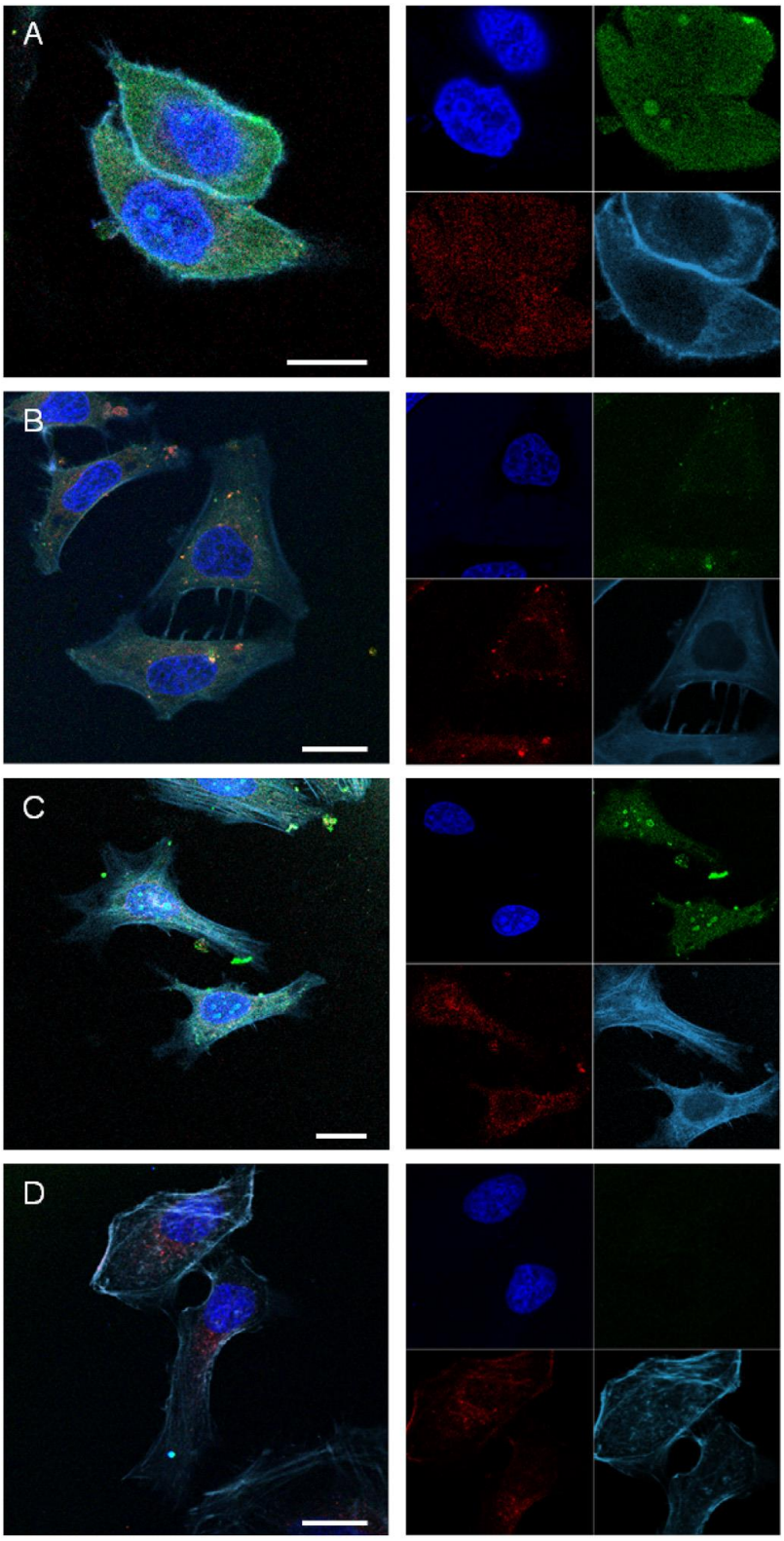

Fig. 12. Confocal microscopy images of HeLa cells after 24 h of treatment with free siRNA and complexes. A - AuNP13 with siMcl-1, B - AuNP14 with siMcl-1, and C - AuNP15 with siMcl-1, D - free siMcl-1. Blue - cell nuclei; red - endosomes; green - FITC-siRNA; cyan -actin filaments. Scale bar= 10 µm.

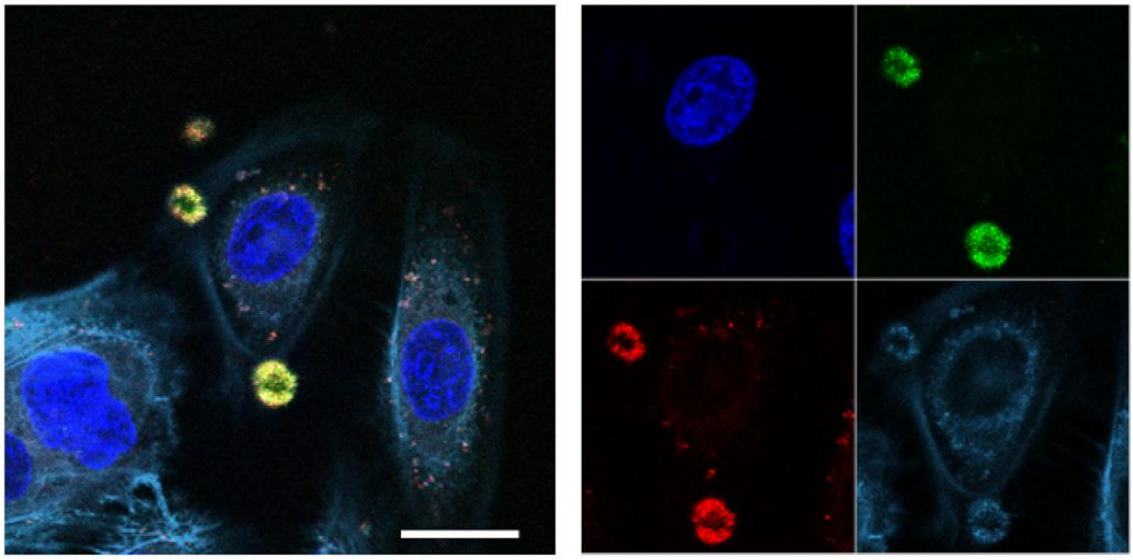

Fig. 13. Confocal microscopy images of HeLa cells after 24 h of treatmentwith the complex of AuNP14 and siBcl-xl. Blue - cell nuclei; red - endosomes; green - FITC-siRNA; cyan -actin filaments. Scale bar= 10 µm.

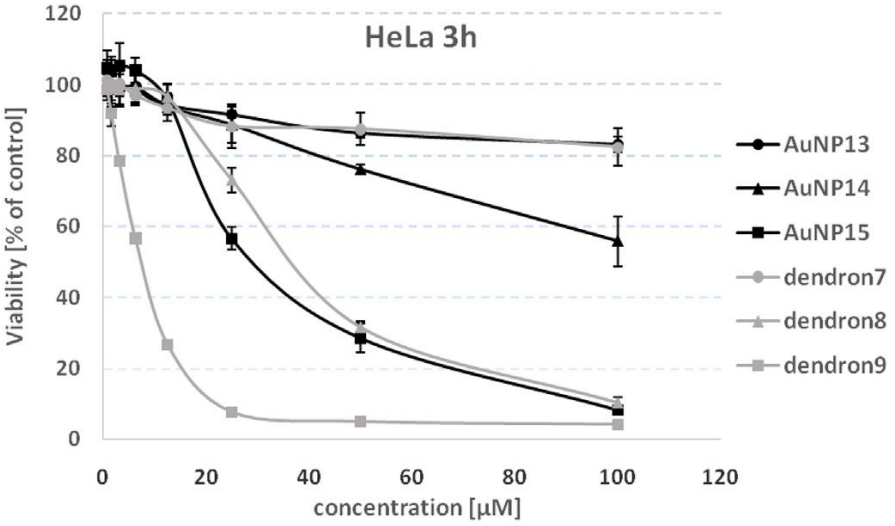

Fig. 14. Cytotoxicity of AuNPs and corresponding dendrons towards HeLa cells. The data given are the means ± SD (n=3).

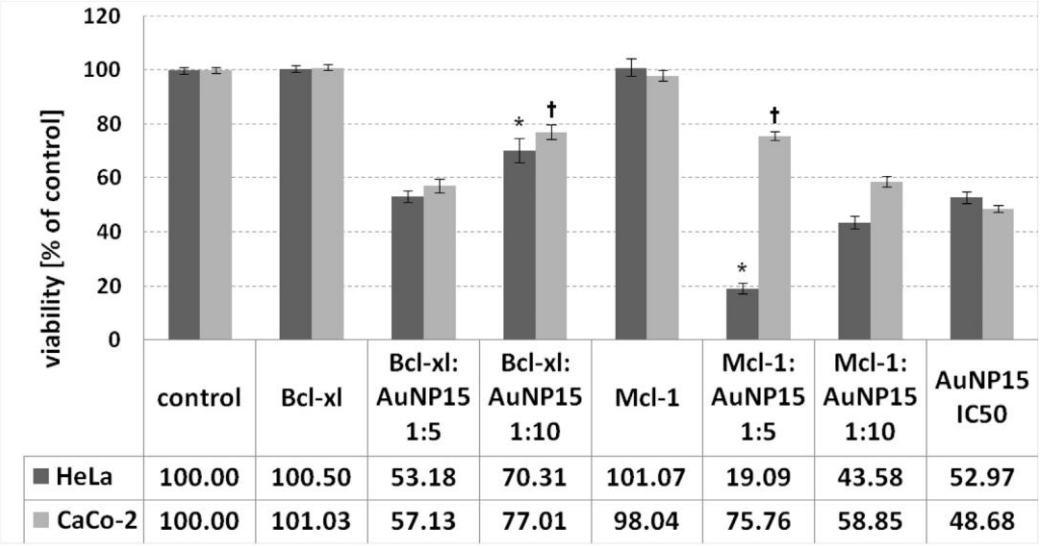

	control	Bcl-xl	Bcl-xl: AuNP15 1:5	Bcl-xl: AuNP15 1:10	Mcl-1	Mcl-1: AuNP15 1:5	Mcl-1: AuNP15 1:10	AuNP15 IC50
HeLa	100.00	100.50	53.18	70.31	101.07	19.09	43.58	52.97
CaCo-2	100.00	101.03	57.13	77.01	98.04	75.76	58.85	48.68

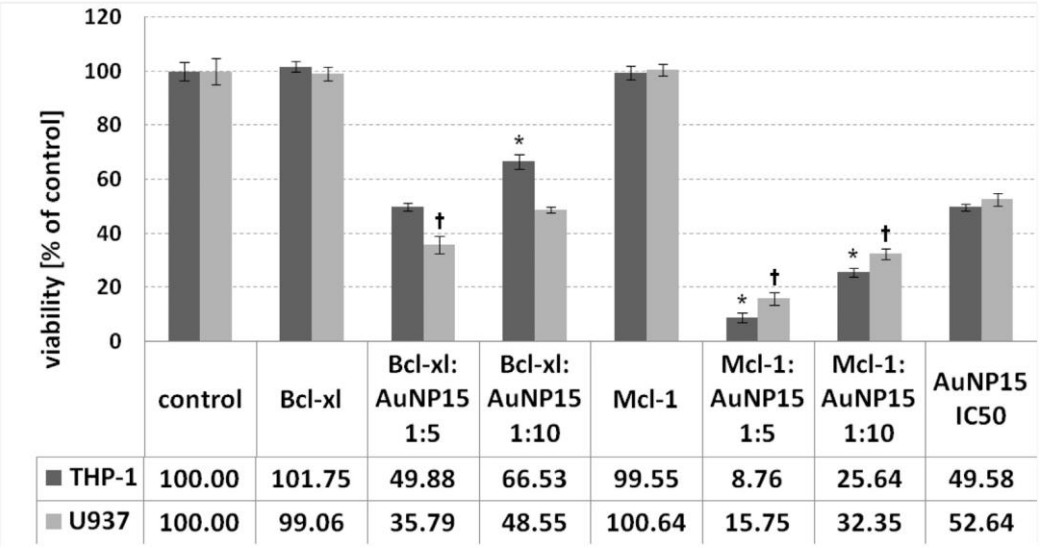

	control	Bcl-xl	Bcl-xl: AuNP15 1:5	Bcl-xl: AuNP15 1:10	Mcl-1	Mcl-1: AuNP15 1:5	Mcl-1: AuNP15 1:10	AuNP15 IC50
THP-1	100.00	101.75	49.88	66.53	99.55	8.76	25.64	49.58
U937	100.00	99.06	35.79	48.55	100.64	15.75	32.35	52.64

Fig. 15 shows that the effect of complexes was similar for all 4 cell lines. The effect of AuNP15:siBcl-xl complex was determined by the effect of the pure nanoparticle. In contrast, the cytotoxicity of complex AuNP15:siMcl-1 for 3 cell lines (HeLa, THP-1, U937) was significantly higher than that of the pure AuNP15.